Flow control of SBLI using grooves with suction

SENTHILKUMAR SUBRAMANIAN
School of Mechanical Engineering
Glasgow University, Glasgow, Scotland, UK
Email- s.subramanian.1@research.gla.ac.uk

KONSTANTINOS KONTIS
School of Mechanical Engineering
Glasgow University, Glasgow, Scotland, UK
Email- kostas.kontis@glasgow.ac.uk

Abstract- Shock wave boundary layer interaction (SBLI) is often encountered in supersonic/hypersonic engine intakes and transonic flow over aerofoil. The interaction of 'strong' shock with turbulent boundary layer can cause the reversal of flow velocity at bottom of the layer. This flow reversal separates the boundary layer from the wall, results in loss of thrust and engine efficiency. One among the proven method to control the flow separation due to SBLI is boundary layer mass suction. This paper discusses the control of SBLI through mass suction in different groove geometries. The 'suction' pressure applied at the bottom of the grooves effectively control flow separation and transforms the complex Type II shock-shock interference into a regular shock reflection. Static pressure rise across SBLI has been reduced to 50% of its peak value irrespective of groove shapes. A complete total pressure recovery has been achieved in 'forward facing triangular' case. A total pressure recovery up to 45% for 'circular' and 55% for 'triangular' has been attained. Among the geometries tested, 'forward-facing triangular' controls flow separation better than the other shapes whereas the 'forward facing blade' controls the least. Reversal of flow velocity inside the gaps of 'triangular' grooves necessitate optimization of groove profile.

Keywords – SBLI, Intakes, Grooves, Shock waves

I. INTRODUCTION

Shock waves occur when there is a sudden deflection in wall boundary towards the incoming supersonic/hypersonic flow. Depends on the flow Mach number, and the shock deflection angle, the shock wave can be either strong or weak. The occurrence of a 'strong' shock in a supersonic flow imparts an adverse pressure gradient across the shock. When interacts with the wall boundary layer, the pressure gradient instigates a catastrophic flow reversal at shock foot and separates the boundary layer from wall. This boundary layer separation often accompanied by large scale unsteadiness which leads to wing buffeting or reduction in engine thrust.[1,2] This phenomenon is termed as SBLI (shock wave boundary layer interaction) in the scientific literature.

The interaction of shock waves on wall boundary layer has always been an active area of interest due to its complex nature. There are multiple ways for a SBLI can occur in high speed flows such as 1) the interaction of a 'strong' shock wave with a laminar/turbulent boundary layer, 2) the ramp flow – where a sudden deflection in the wall geometry towards the incoming supersonic flow creates a series of shock waves originating from the wall boundary layer and 3) the transonic flow over an aerofoil or a 3-dimensional bump.[3]

Controlling SBLI in high-speed flow can be achieved either by modifying the strength of the originated shock or by modifying the structure of boundary layer ahead of the interaction.[4] Depending on the need, either the shock control or the boundary layer control can be chosen as both have their inherent advantages in controlling flow separation and reducing stagnation pressure loss respectively. Mass blowing, mass suction, and vortex generators (VG) are the boundary layer control methods used in controlling flow separation due to SBLI.[5] In this paper, Mass suction through differently shaped grooves was considered and the results are presented. The results show the groove profile has a distinct effect on controlling flow separation. The simulation was done in commercially available flow analysis software STAR CCM +.

II. Computational Work

2.1 CAD Design

A 2-dimensional Computer Aided Design model of high-speed 'intake wind tunnel' test section was designed as per the dimensions in figure 1. The location of grooves at the lower wall is chosen to be compatible with the existing wind tunnel test section windows location in Glasgow university. This will allow us to collate the computational results with experimental results in the future. Suction pressure was applied at the base of the grooves as shown in the enlargement in figure 1. The groove shapes considered for the study are presented as an inset in figure 1. The dimensions of the grooves are inspired by the work published at Embry-Riddle Aeronautical University.[6] The dimensions are fixed at (depth) a = 7.5mm, (spacing) b = 5mm and (thickness) c = 2.5mm for all the cases. A 2D wedge is introduced to create a strong shock inside the test section. The location of the 2D wedge is selected such that the shock emerging from the wedge fall on top of the grooves and also the suction produced on the windward side of the SBLI has a greater effect on controlling flow separation along the groove wall.[7]

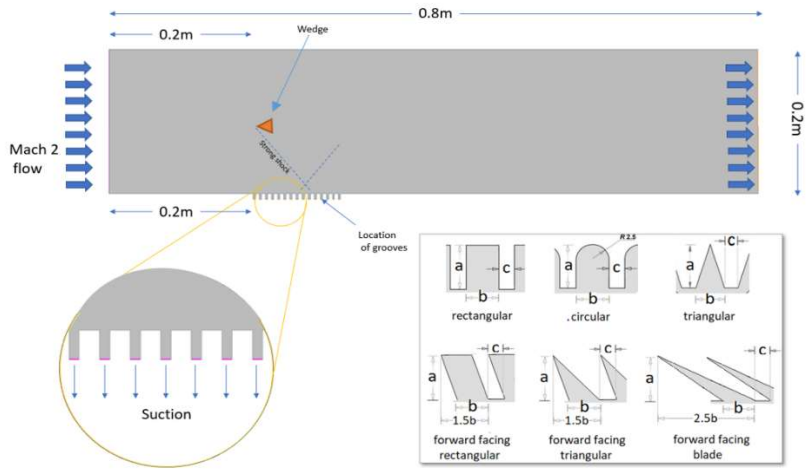

Fig. 1 – 2D CAD model of intake wind tunnel test section fixed with rectangular grooves (Inset picture –groove shapes considered in this study)

2.2 Meshing

Trimmer, Surface remesher, and Prism layer are the meshing models involved to create mesh in STAR CCM+. Trimmer is one of the three types of volume mesh available in the software, the other two are polyhedral and tetrahedral. However, the choice of the trimmer is made since it is independent of the model quality and gives a computationally efficient, accurate solution for a given volume compared to the other two.[8] Also, the alignment of mesh with the flow direction will reduce numerical dissipation. The meshing was originally constructed as 3D and later converted to a 2D mesh as the test section flow field is assumed to be 2 dimensional. The base size of the mesh is selected as 0.5mm which provides enough node points inside a groove thickness of 2.5 mm. The maximum cell size is 200% of its base size. The resultant mesh for rectangular groove is presented in fig 2.

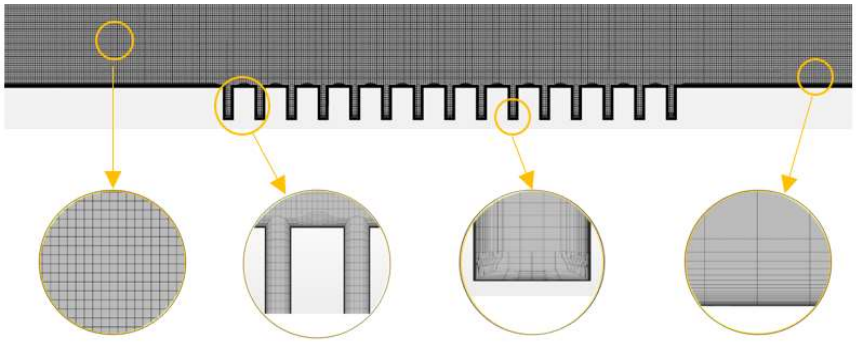

Fig. 2 – 2D mesh of test section with rectangular grooves

2.3 Physical model

The physical model needed for the simulation is selected based on the isentropic compressible flow assumptions. The flow is assumed to be two dimensional, steady, and non-reacting Ideal gas. Star CCM+ offers two types of solver - coupled and segregated. Although coupled solver needs high computational power compared to segregated, the accuracy in compressible flow problems can be achieved by coupled solver as it solves the continuity and momentum equation simultaneously.[8] Hence coupled flow solver is chosen for the simulation. K-epsilon turbulent model is chosen as this suit for high Reynolds number, predicting turbulent shear flows and gives standard results.[9]

The stagnation pressure to achieve Mach 2 flow is calculated from eq (1) and the calculated stagnation and reference static pressure values as in table (1) are entered as inputs in the software.

$$\frac{P_0}{P} = \left(1 + \left(\frac{\gamma-1}{2}\right) M^2\right)^{\frac{\gamma}{\gamma-1}} \quad (1)$$

Mach Number	Temperature (K)	Dynamic viscosity ($N/m^2.s$)	Density (Kg/m^3)	$\frac{P}{P_0}$	Total Pressure P_0 (N/m^2)	Static Pressure Reference P (N/m^2)
2	303 K	0.0000188606	1.16439	0.12780452	88375.20701	12949.79299

Table. 1

III. RESULT

3.1 Computational Results

The static pressure distribution with and without suction control for Mach 2 supersonic flow is presented in fig (3). Flow over 'without suction' indicates the development of SBLI along the bottom wall, whereas the rest of the groove geometries with activation of 'suction' eliminates the SBLI from bottom wall and converts the complex shock-shock interaction into a regular reflection.

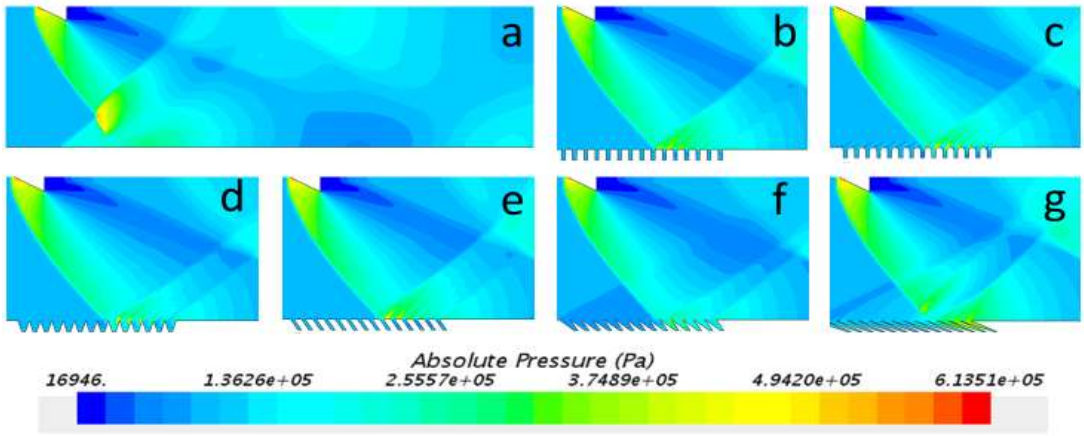

Fig. 3 – Static Pressure distribution
a-without suction, b-suction in rectangular grooves, c-suction in circular grooves, d-suction in triangular grooves, e-suction in forward-facing rectangular grooves, f- suction in forward-facing triangular grooves, g- suction in forward-facing blades

The close-up image of velocity vector distribution for 'no suction' case reveals the development of a 'separation bubble' and the reversal of boundary layer flow velocity at the bottom wall (fig. 4a). The inflow of high pressure behind the refracted shock into the subsonic boundary layer promotes a reverse flow along the bottom of the wall. The pressure rise caused by the flow reversal creates a 'separation bubble' inside the subsonic boundary layer which acts as a virtual bump to the incoming flow. The sudden deflection of flow velocity due to 'virtual bump' instigate a separation shock ahead of the bump. Based on the incident shock strength, the intersection with the separation shock can be either a Type I shock/shock interference (regular reflection) or a Type II interference (normal shock connecting the incident and separation shock to create a Mach reflection) as shown in figure 4b.[10]

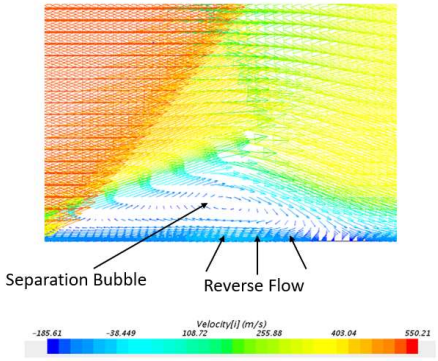

4a -X-velocity vector distribution 'no suction' case

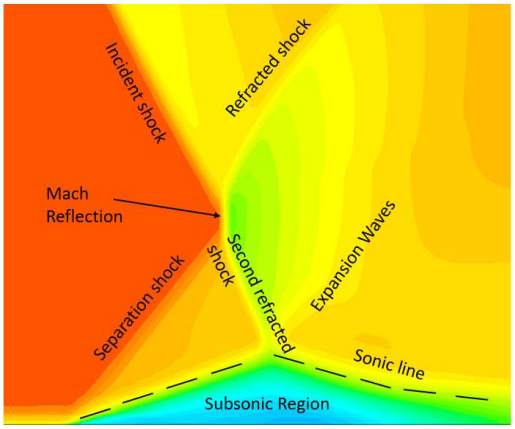

4b – X-velocity distribution for Type II Interference

To investigate the flow properties at the core of boundary layer separation, a 'line of interest' 2mm above the top of the grooves is drawn in STAR CCM+ as shown in fig (5). The line starts 5 cm ahead of the grooves and completely covers the groove section and extends up to 10 cm aft the end of grooves. The 'line of interest' covers approximately 30% of the total test section length.

Fig. 5 – 'Line of interest' for plotting flow properties

The static pressure along the 'line of interest' is plotted in fig (6). The steep rise in the pressure at 0.19 m for the case 'without suction' and subsequent pressure rise around 0.24m shows the presence of a 'separation shock' and a 'refracted shock' due to the separation bubble. Then the static pressure decreases gradually as it passes through a series of expansion waves. Among the groove cases, 'forward-facing blade' causes pressure rises due to the tendency of flow separation at sharp edges in blades. The rest of the 'grooves with suction' cases minimize SBLI effectively by reducing the separation bubble and eliminating separation shock. However, it is observed that there is a pattern of minor pressure fluctuations for all the groove cases as seen in fig (6). This is due to the simultaneous shock and expansion waves originating from the individual groove tip.

The stagnation/total pressure changes along the 'line of interest' are presented in fig (7). In an inviscid, shock-free isentropic flow, the total pressure is assumed to be conserved as in the flow inside constant area duct. But the introduction of a sudden deflection in the wall boundaries in the form of wedge or grooves creates shock waves which result in total pressure loss. Also, the act of suction draws out a small percentage of fluid from the subsonic boundary layer near the groove wall and cause additional total pressure loss.[11] As expected, 'without suction' case encounter a sudden loss in total pressure due to the 'separation shock' and 'refracted shock' present in SBLI. Among the grooves, suction coupled with 'forward-facing triangular' grooves recovers total pressure better compared to other cases as seen in fig (7). At sharp corners or at sudden high angled wall deflection, a free shear layer will be formed as the vorticity contained in the boundary layer separates from the surface.[12] This can be attributed by the huge total pressure loss in 'forward-facing blades'. The same trend (total pressure loss) can also be witnessed in 'circular' grooves and 'triangular grooves' as both have sudden high angled deflection to the incoming flow.

Mach number variation along the 'line of interest' is plotted in fig (8). The case 'without suction' and 'forward-facing blade' decelerate the flow quickly into the subsonic (M<1) region. In contrast, the 'forward-facing triangular' groove maintains a gentle Mach number decrease in the supersonic regime as the flow progress. The 'rectangular' and 'forward-facing rectangular' also shows a similar trend. The amplitude variation in Mach number for the 'circular' grooves is due to the simultaneous shock-expansion formation on the curved profile of the groove tip.

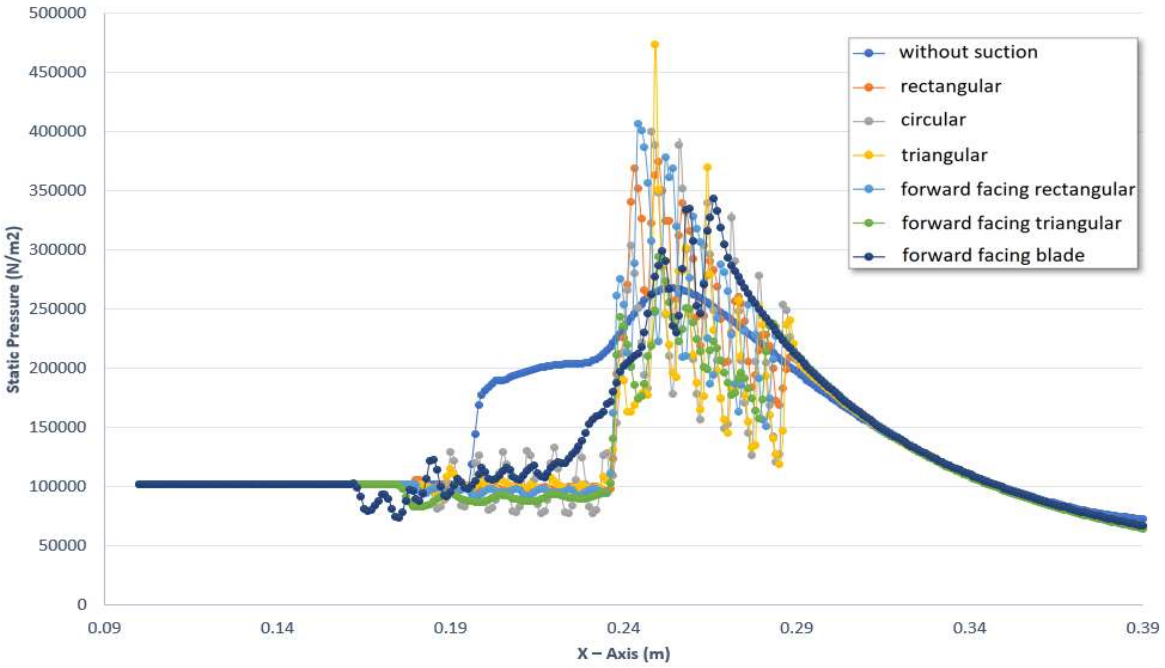

Fig. 6 –Static Pressure distribution along the line of interest

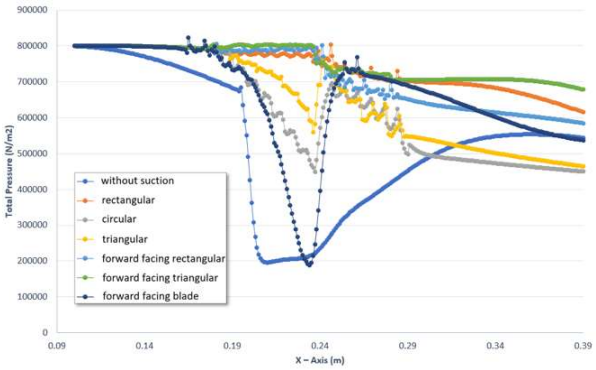

Fig. 7 – Stagnation/Total pressure distribution

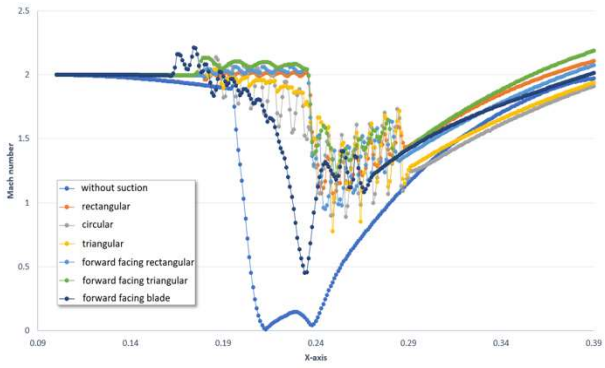

Fig. 8 – Mach number distribution

The Mach number distribution in fig (9a) shows the subsonic flow behind Type II shock-shock interaction for 'without suction'. Shock waves of different strength influenced by the groove shapes can be seen from 9b to 9g. There is a noticeable reduction in the shock angle of reflected shock for 'forward-facing triangular' groove configuration. Reduction in shock angle can be related to decrease in (reflected) shock strength which explains the recovery of pressure loss as earlier seen in fig (7). The Mach number reduced to almost zero in between the groove space and at the foot of SBLI where flow separation occurs. Also, the lucid representation of color plots indicates the region of subsonic flow in areas behind bow shock and behind the wake of the wedge model.

The comparison of X-velocity distribution is presented in figure (10). Unlike the 'no suction' case, the flow reversal and associated flow separation are successfully controlled in all the groove cases. However, it is interesting to note the influence of the groove upper wall profile on the flow velocity direction. The aft side of 'triangular grooves' and the front face of 'sweep forward triangular' grooves experience a reversal of flow velocity as shown in the enlarged picture in fig (10). This indicates the need for optimization of the groove shapes for efficient flow control.

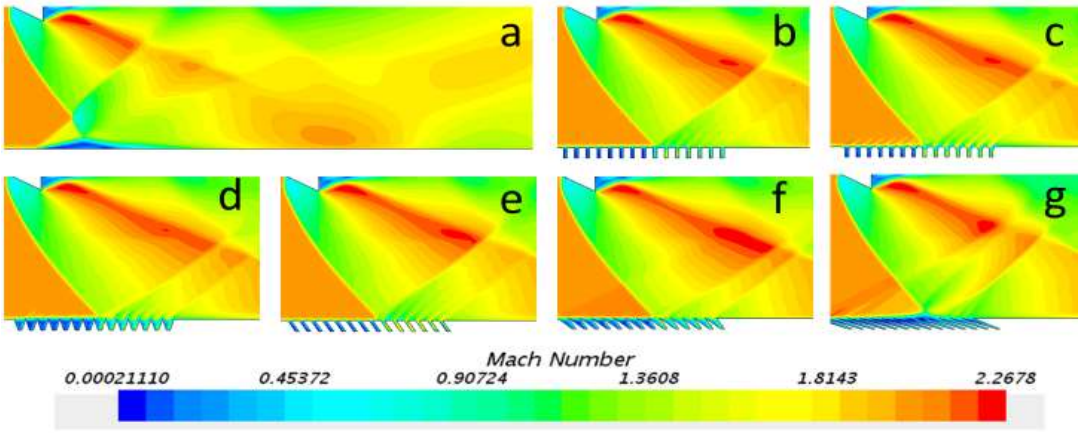

Fig. 9 – Mach number distribution
a-without suction, b-suction in rectangular grooves, c-suction in circular grooves, d-suction in triangular grooves, e-suction in forward-facing rectangular grooves, f- suction in forward-facing triangular grooves, g- suction in forward-facing blades

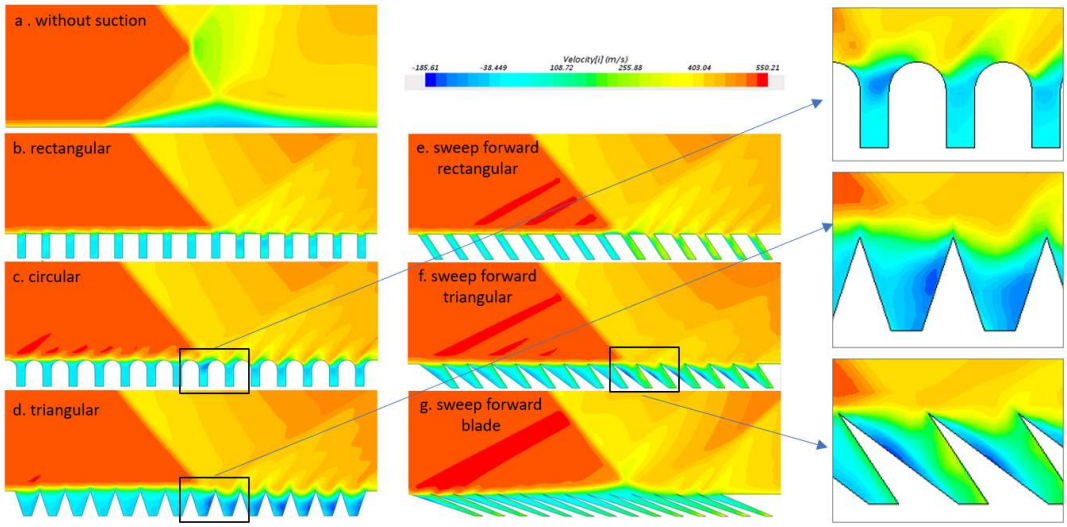

Fig.10 – X-velocity vector distribution for differently shaped grooves with suction

The vector field inside the grooves can be effectively visualized by using the velocity integral convolution option available in STAR CCM +. The vector field inside the rectangular grooves without the activation of suction in fig (11) shows the presence of clockwise and anticlockwise circulation inside the confined space. The rotational velocity and size of the circulation vary on subsequent grooves. The presence of circulation also can be seen in suction cases. The circulation size and structure are more influenced by the profile of the grooves as observed in fig (10).

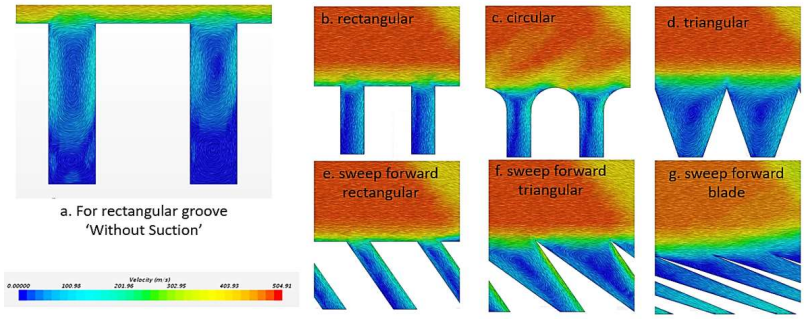

Fig. 11 – Visualization of vector field inside different grooves

To investigate the flow properties along the cross-section of the test section, a line of interest at 1 cm behind the wedge model is created in STAR CCM+ as shown in fig (12 a). The comparison of X- velocity distribution along the cross-section of the test section shows the distinct reverse flow region near to the bottom of the wall for 'without suction'. However, the reverse flow has been controlled from creating flow separation when the suction control is 'on' for the rest of the cases as seen in fig (12b).

The total pressure loss due to boundary layer flow separation for the 'no suction' has been recovered well by suction along with grooves as seen in figure (13). The static pressure distribution along the 'line of interest' is plotted in fig (14). It reveals the case 'without suction' yield raise of pressure up to 5 bar due to presence of Mach reflection. However, grooves with suction reduces the pressure to 2.5 bar, which account for 50% reduction from 'no suction' case. On comparing the effect of shapes in controlling SBLI, the suction in 'forward-facing triangular' groove controls SBLI much better, whereas the suction in 'forward-facing blade' groove controls the least. The performance of controlling SBLI by 'forward-facing triangular' is proved again in both fig (13) and (14).

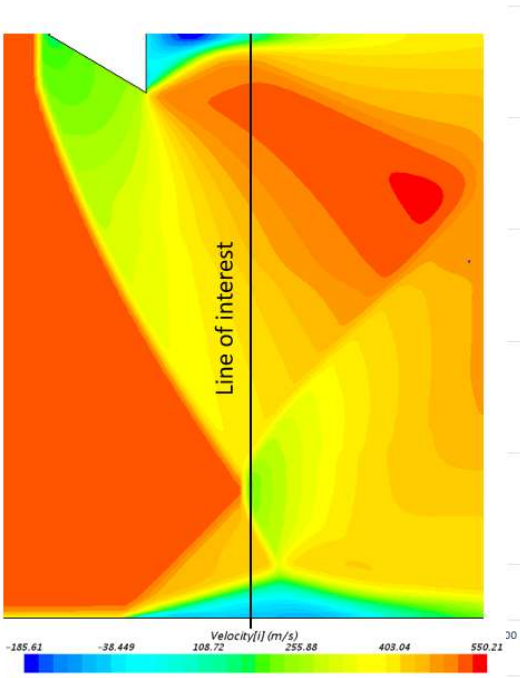

Fig.12a

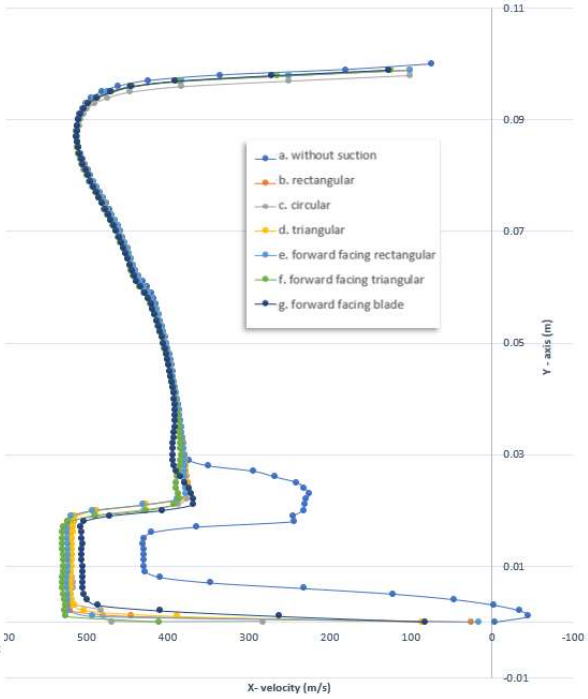

Fig.12b

X-velocity distribution along the 'line of interest'

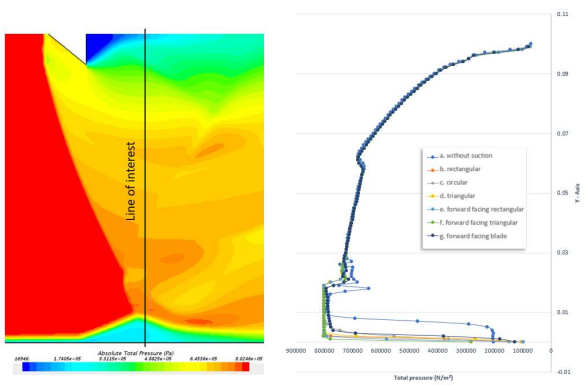

Fig. 13 -Total pressure variation

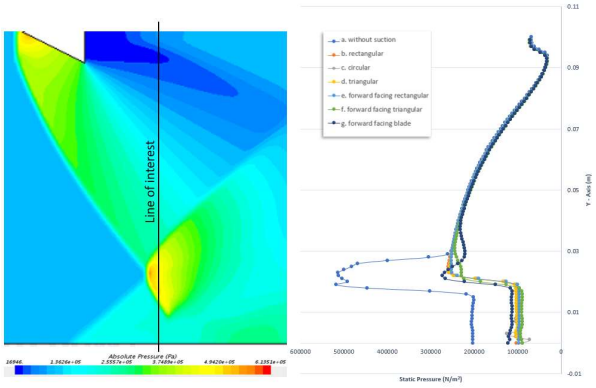

Fig. 14 -Static pressure variation

IV.CONCLUSION

Controlling SBLI has been a challenge for many years since it accounts for the loss in high-speed engine intake efficiency and loss of lift in transonic flights. Different types of groove geometries with suction control are considered in this paper to suppress the formation of SBLI induced flow separation. The grooves fitted test section has been designed and simulated in STAR CCM+. The physical conditions are given to achieve Mach 2 in the test section and vacuum pressure at the base of the grooves.

The activation of 'suction' pressure along with the grooves effectively control SBLI by removing the formation of separation bubble in the wall boundary. The loss of total pressure from the separation shock, which accounts for a major part of overall drag, has been recovered completely in 'forward-facing triangular' groove. Loss in total pressure up to 45% for 'circular' and 55% for 'triangular' has been recovered. The reduced performance in total pressure recovery in 'forward-facing blade' is attributed to the formation of a shear layer due to separation of vorticity at sharp corners. The variation of Mach number shows a similar trend as total pressure. The Mach number reduced to subsonic values due to flow separation in 'forward facing blade'.

Minor fluctuations of pressure values have been witnessed along the length of the grooves due to simultaneous shock-expansion formation on the profile of the groove tips. The fluctuations are more pronounced in sharp-edged groove tips than a rounded one. Reduction in shock strength benefitted from the reduced shock angle in 'forward faced triangle' has been observed. Surprisingly, the reversal of flow velocity has been observed in the gaps of 'triangular' shaped grooves. This indicated the need of groove shape optimization for efficient flow control.

The activation of suction pressure not only control SBLI induced flow separation but also transform the complex Type II shock-shock interference into a regular shock reflection. Overall, the performance of 'forward-facing triangular' is comparatively better than other shapes. The 'forward-facing blade' shape offers the least performance due to flow separation caused at the tip of acute sharp angles. Static pressure reduction up to 50% of its peak value has been achieved irrespective of groove shapes. The total pressure loss due to SBLI has been well recovered. The activation of 'suction' at the bottom of grooves promises good control effectiveness of flow separation due to shock interference.

V. REFERENCES

[1] Délery, Jean, and Jean-Paul Dussauge. "Some physical aspects of shock wave/boundary-layer interactions." *Shock waves* 19, no. 6 (2009):

[2] Gaitonde, Datta V. "Progress in shock wave/boundary layer interactions." *Progress in Aerospace Sciences* 72 (2015): 80-99.

[3] Délery, J., and R. Bur. "The physics of shock wave/boundary-layer interaction control: last lessons learned." *OFFICE NATIONAL D ETUDES ET DE RECHERCHES AEROSPATIALES ONERA-PUBLICATIONS-TP* 181 (2000).

[4] Babinsky, Holger, and Hideaki Ogawa. "SBLI control for wings and inlets." *Shock Waves* 18, no. 2 (2008): 89.

[5] Pearcey, H.H.: Shock-induced separation and its prevention by design and boundary layer control. In: Boundary Layer and Flow Control, vol. 2, pp 1166–1344. Pergamon Press, (1961).

[6] Seyed Mehdi Mortazawy, Konstantinos Kontis and John A. Ekaterinaris., "A Numerical Investigation of Shock Wave Propagation in Ducts with Grooves" AIAA 2019-2152, 6 Jan 2019.

[7] Yan, Li, Han Wu, Wei Huang, Shi-bin Li, and Jun Liu. "Shock wave/turbulence boundary layer interaction control with the secondary recirculation jet in a supersonic flow." *Acta Astronautica* (2020).

[8] Karakas, Hakki, Emre Koyuncu, and Gokhan Inalhan. "ITU tailless UAV design." *Journal of Intelligent & Robotic Systems* 69, no. 1-4 (2013): 131-146.

[9] Argyropoulos, C. D., and N. C. Markatos. "Recent advances on the numerical modelling of turbulent flows." *Applied Mathematical Modelling* 39, no. 2 (2015): 693-732.

[10] Edney, B. "Anomalous heat transfer and pressure distribution on blunt bodies at hypersonic speeds in the presence of an impinging shock.-The Aeronautical Research Institute of Sweden, Stockholm FFA Rep. 115." (1968).

[11] Kang, K., L. Wermer, S. Im, S. J. Song, and H. Do. "Fast-Acting Boundary-Layer Suction to Control Unstarting and Unstarted Flows." *AIAA Journal* (2020): 1-11

[12] C. A. M., and H. W. M. Hoeijemakers. "A vortex sheet method applied to unsteady flow separation from sharp edges." *Journal of Computational Physics* 120, no. 1 (1995): 88-104.